Supporting information

In-situ study of catalytic CO oxidation on ultrathin MgO film supported Pd nanoparticles by Sum frequency generation: size and site effect

Jijin Wang, Aimeric Ouvrard, Wanquan Zheng, Serge Carrez, Ahmed Ghalgaoui and Bernard Bourguignon*

Institut des Sciences Moléculaires d'Orsay, CNRS, Université Paris-Saclay, 91405, Orsay, France

Corresponding author : E-mail: wangjij@lzu.edu.cn

1. Non resonant SFG response of O-Pd NPs interaction

Because the Pd-O vibration frequency (445, 651 cm^{-1} [**1**,**2**]) cannot be reached with our SFG apparatus, to follow Pd-O interaction on Pd surface by SFG, an indirect way consists in comparing the variation of the SFG non-resonant (NR) signal on Pd surface during atomic O adsorption. NR SFG signal originates mostly from the off-resonant transitions near the Fermi energy level of the substrate that can be modified by molecular adsorption [**3**].

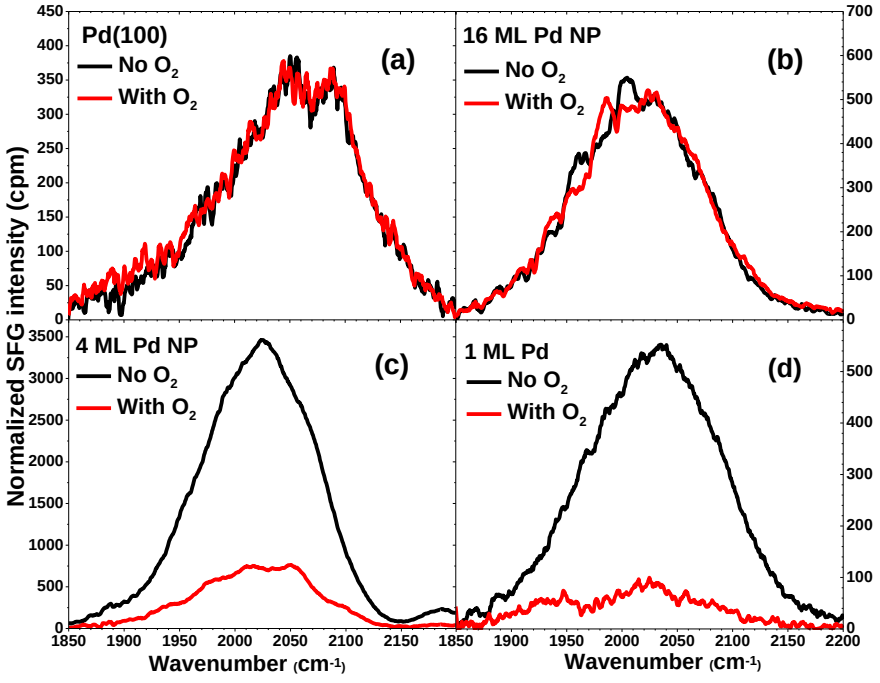

Figure S1. NR SFG spectra without (black) and with (red) 1×10^{-4} mbar O_2 exposure on (a) Pd(100) single crystal, (b) coalesced; (c) 5.8 nm and (d) 3.6 nm average diameter Pd NPs on MgO/Ag(100) at 293 K.

As shown in Figure S1 on (a) Pd(100) single crystal and (b) 16 ML coalesced Pd NPs, the presence of 10^{-4} mbar O_2 do not change SFG non-resonance (NR) signal, however the NR is strongly reduced on 4 and 1 ML Pd NPs. Because at 293 K O_2 can already dissociate, the large decrease of NR signal on small Pd NPs, but not on Pd single crystal or coalesced Pd surface, cannot be attributed to presence of O(ad). In fact, it has been shown by molecular beam techniques that oxygen can be incorporated in the volume of the Pd clusters already below 300 K [**4**], and O migration into Pd(111) single crystal subsurface does not happen at room temperature and below [**5,6**], the strong decrease of NR for small Pd NPs is therefore attributed to incorporated subsurface O atoms.

2. Calculation of CO adsorption and oxidation rates:

In Figure S2, if we call the CO adsorption rate $a_{CO,}$ the CO desorption rate d_{CO}, the CO oxidation rate σ_{O+CO}, then the expression for the surface CO coverage variation rate $d\theta_{CO}/dt$ is:

$$\frac{d\theta_{CO}}{dt} = a_{CO} - d_{CO} - \sigma_{O+CO} \qquad (1)$$

Without oxygen in the chamber, the CO band frequency on Pd(100) would be kept at 1950 cm^{-1} [**7**]. However when O_2 is present under a constant pressure of 10^{-5} mbar, the reaction depletes completely the surface from 0.5 ML CO within 1 min under a CO pressure of 10^{-9} mbar or within 1.5 min under a CO pressure 10^{-8} mbar, indicating that the σ_{O+CO} is much larger than d_{CO} at 293 K.

In the first measurement because a_{CO} is very small under a pressure of 10^{-9} mbar [**7**] and σ_{O+CO} is much larger than d_{CO}, we can estimate σ_{O+CO} to be approximately 0.5 ML·min^{-1}. In the second case when the CO pressure is decreased from 10^{-7} mbar to 10^{-8} mbar, the CO coverage decreases from 0.5ML to 0 ML within 1.5 min, deducing σ_{O+CO} - a_{CO} is 0.5 ML per 1.5 min = 0.33 ML·min^{-1}. This longer time of disappearance of the CO band should be caused by the non-negligible CO adsorption rate a_{CO} under 10^{-8} mbar. Comparing with the oxidation rate of CO obtained from the first measurement, a_{CO} under a pressure of 10^{-8} mbar is thus determined to be approximately 0.17 ML.min^{-1}. This value corresponds to an average sticking coefficient of ~0.25 over the whole coverage range, which is quite reasonable.

3. SFG results of CO oxidation on Pd(100)

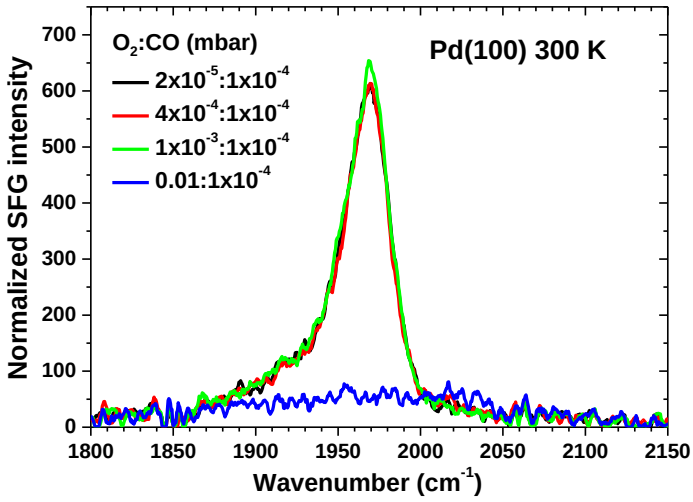

Figure S2. SFG spectra of CO (10^{-4} mbar) adsorbed on O_2 pre-treated (10^{-4} mbar O_2 for 20 min) Pd(100) single crystal as a function of O_2 pressure from 10^{-5} up to 0.01 mbar at 293 K.

CO oxidation on Pd(100) are shown in Figure S2 and can be referred with CO oxidation on coalesced Pd NPs in Figure 2a. CO band intensity keeps constant when the O_2 pressure is increased to 10^{-3} mbar, and then suddenly vanishes when O_2 pressure reaches 0.01 mbar.

4.AFM Characterization of Pd Nanoparticles

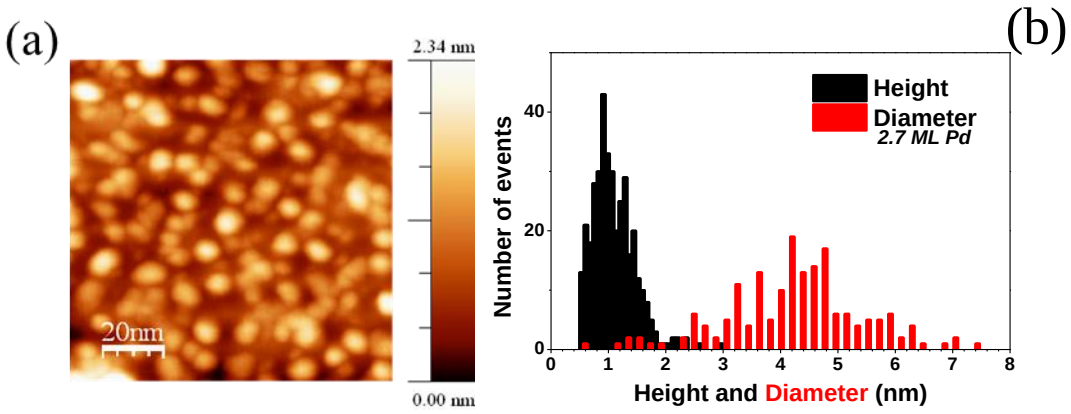

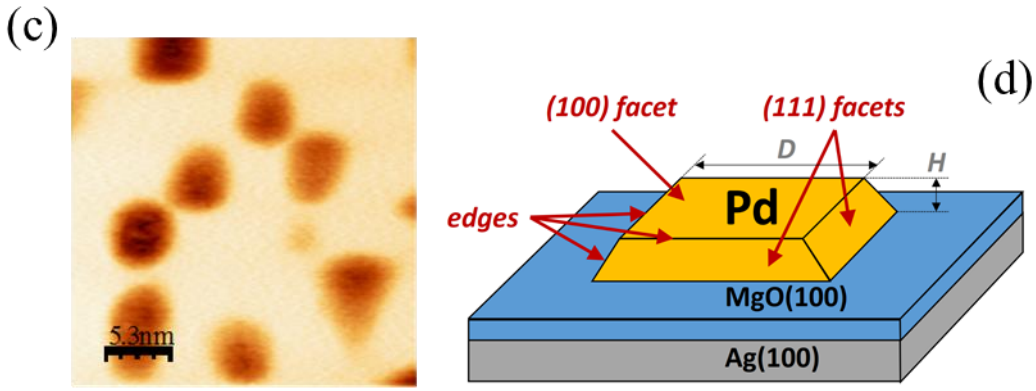

Figure S3. (a) noncontact-AFM (nc-AFM) topography image (100×100 nm^2) of 2.7 ML Pd on a 3 ML MgO film. The density of NP is ~1.6±0.3×10^{12} cm^{-2} covering 35% of the MgO film. (b) Height and diameter statistics extracted from part a after removing tip convolution. (c) AFM constant height mode image (30×30 nm^2). The NPs' top facet are square, as expected from their known truncated octahedron shape and considering the (100) crystalline orientation of the substrate. The measured aspect ratio (width/height) is around 4:1±0.5. (d) Schematic representation of a Pd NP on the ultrathin MgO film. This figure is from Figure 1 in ref. [8].

A nc-AFM topography image obtained on a 2.7 ML thick Pd film is shown in Figure S3a [8]. The substrate temperature is kept at 473 K during the deposition. Randomly distributed NPs with a high density of 1.6 ± 0.3 × 10^{12} NPs/cm^2 can be found. A reasonably narrow size distribution of ±20% is observed (Figure S3b). We use the constant height mode of the nc-AFM to image the shape of the NP's top facets with a tip−surface convolution almost at zero (Figure S3c). The NP shape is known to be a truncated octahedron and we find an aspect ratio (width/height) of 4:1 ± 0.5. Because of the specific epitaxy on the MgO(100) substrate, the observed flat terrace orientation is mostly (100) as it can be indeed seen in Figure S3d. In Table S1 the geometrical parameters of Pd NPs for various equivalent thicknesses of Pd deposits are summarized. These values are extrapolated from the nc-AFM images in Figure S3, assuming that the size aspect ratio is not size dependent [8].

5. Calculation of terrace/edge ratio of NP

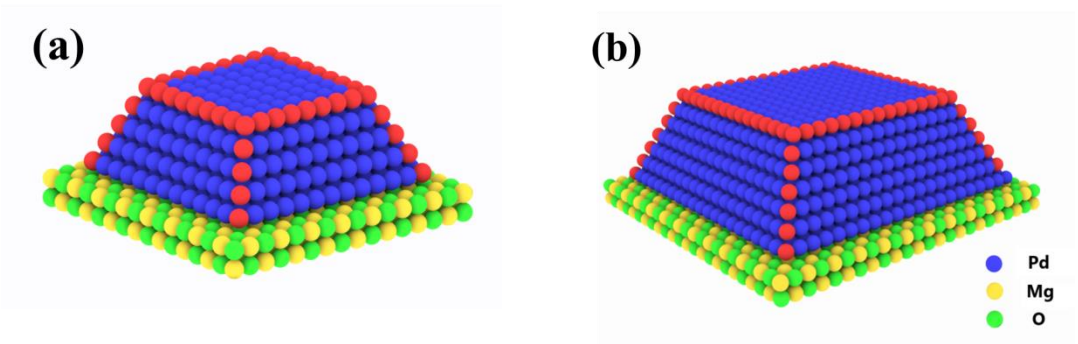

Figure S4. Sketch of (a) 3.6 nm and (b) 5.8 nm average diameter Pd NPs on MgO(100).

5.8 nm average diameter NP is chosen as a sample for terrace/edge calculation. Considering the distance between Pd atoms on (100) facet 0.28 nm, a height of 6-9 monolayer, the width of the top facet is 3.6-4.4 nm [8], with 14-17 edge atoms between terrace and every side facet, and 5-8 edge atoms between side facets, $N_{terrace}/N_{edge}$ can be obtained 2.3±0.5. The details of NP parameters of 3.6 and 5.8 nm Pd NPs are shown in Table S1.

Table S1. Estimated diameter, height, total (N_{Total}), facet (N_{Facet}), terrace($N_{Terrace}$), edge(N_{Edge}) atom number and atom ratio of terrace to edge for different equivalent thicknesses of Pd assuming a constant D/h aspect ratio. [a] coalesced NPs.

Pd (ML)	Diameter (nm)	Height (nm)	Height (ML)	N_{Total}	N_{Facet}	$N_{Terrace}$	N_{Edge}	$N_{terrace}/N_{edge}$
1	3.6 ± 0.4	0.9 ± 0.2	4−6	820 ± 380	210 ± 40	65 ± 15	48	1.3±0.3
4	5.8 ± 0.6	1.5 ± 0.3	6−9	3300± 1380	550 ± 90	180 ± 40	80	2.3±0.5
16[a]	-	3.1 ± 0.1[a]	16[a]	-	-	-	-	-

References:

[1] McBride J. R., Hass K. C., and Weber W. H., Resonance-Raman and lattice-dynamics studies of single-crystal PdO, *Phys. Rev. B*, 44, 5016

[2] Chlebda D. K., Jędrzejczyk R. J., Jodłowski P. J., Łojewska J., Surface structure of cobalt, palladium, and mixed oxide‐based catalysts and their activity in methane combustion studied by means of micro‐Raman spectroscopy, *J Raman Spectrosc.*, **2017**, 48, 1871–1880

[3] Morkel M., Unterhalt H., Klüner T., Rupprechter G., Freund H.-J., Interpreting intensities in vibrational sum frequency generation (SFG) spectroscopy: CO adsorption on Pd surfaces, *Surf.Sci*, **2005**, 586, 146

[4] Meusel I., Hoffman J., Hartmann J., Heemeir M., Baumer M., Libuda J., Freund H.-J., The interaction of oxygen with alumina-supported palladium Particles, *Catal. Lett.* **2001**,71, 5

[5] Leisenberger F.P., Koller G., Sock M., Surnev S., Ramsey M. G., Netzer F.P., Klötzer B., Hayek K., Surface and subsurface oxygen on Pd(111), *Surf. Sci.,* **2000**, 445, 380.

[6] Wrobel R. J., Becker S., and Weiss H., Influence of Subsurface Oxygen in the Catalytic CO Oxidation on Pd(111), *J. Phys. Chem. C*, **2015**, 119, 5386.

[7] Ouvrard A., Wang J. , Ghalgaoui A. , Nave S. , Carrez S. , Zheng W. , Dubost H. , and Bourguignon B., CO Adsorption on Pd(100) Revisited by Sum Frequency Generation: Evidence for Two Adsorption Sites in the Compression Stage, *J. Phys. Chem. C,* **2014**, 118, 19688.

[8] Ouvrard A., Ghalgaoui A., Michel C., Barth C., Wang J., Carrez S., Zheng W., Henry C. R., and Bourguignon B., CO Chemisorption on Ultrathin MgO-Supported Palladium Nanoparticles, *J. Phys Chem. C*, **2017**, *121*, 5551–5564.